

# Improved Deep Reinforcement Learning with Expert Demonstrations for Urban Autonomous Driving

Haochen Liu, Zhiyu Huang, *Student Member, IEEE*, and Chen Lv, *Senior Member, IEEE*

**Abstract**—Currently, urban autonomous driving remains challenging because of the complexity of the driving environment. Learning-based approaches, such as reinforcement learning (RL) and imitation learning (IL), have indicated superiority over rule-based approaches, showing great potential to make decisions intelligently, but they still do not work well in urban driving situations. To better tackle this problem, this paper proposes a novel learning-based method that combines deep reinforcement learning with expert demonstrations, focusing on longitudinal motion control in autonomous driving. Our proposed method employs the soft actor-critic structure and modifies the learning process of the policy network to incorporate both the goals of maximizing reward and imitating the expert. Moreover, an adaptive prioritized experience replay is designed to sample experience from both the agent’s self-exploration and expert demonstration, in order to improve the sample efficiency. The proposed method is validated in a simulated urban roundabout scenario and compared with various prevailing RL and IL baseline approaches. The results manifest that the proposed method has a faster training speed, as well as better performance in navigating safely and time-efficiently. The ablation study reveals that the prioritized replay and expert demonstration filter play important roles in our proposed method.

**Index Terms**—Autonomous driving, deep reinforcement learning, expert demonstrations, urban condition.

## I. INTRODUCTION

RECENT years have witnessed a big leap in the development of autonomous driving techniques, moving from academic progress to practical use [1], [2]. Nevertheless, autonomous driving in urban scenarios remains a major challenge [3], primarily due to the complicated driving conditions, including great variance of traffic density and agent interactions, as well as the requirement of balance between efficiency (speed), comfort (smooth), and safety [4]. Current motion control strategies concentrate on the rule- or model-based methods [5]. These methods excel in interpretability but are with several drawbacks that could impede their application in urban scenarios. First of all, the rules or models are designed manually with potentially inaccurate assumptions, thus making it hard to scale to complicated real-world environments. Moreover, the rules themselves are hard to define and maintain for continual improvement.

This work was supported by the SUG-NAP Grant (No. M4082268.050) of Nanyang Technological University, Singapore.

H. Liu is with School of Mechanical and Aerospace Engineering, Nanyang Technological University, Singapore, and the School of Automation Science and Electrical Engineering, Beihang University, Beijing, China. (E-mail: haochen\_liu99428@163.com)

Z. Huang and C. Lv are with the School of Mechanical and Aerospace Engineering, Nanyang Technological University, 639798, Singapore. (E-mails: zhiyu001@e.ntu.edu.sg, lyuchen@ntu.edu.sg)

Corresponding author: C. Lv

To properly tackle the challenges, we employ a model-free method that learns to control the vehicle from expert demonstrations and the agent’s self-experiences. With the recent breakthroughs in deep learning and deep reinforcement learning, the end-to-end driving framework, which takes as input the state of the driving scene and outputs the motion controls directly, is becoming viable. With diverse driving data, the learning-based method can handle large state and action spaces and complicated situations in urban driving scenarios. In essence, there are two paradigms to learn the motion control strategies, namely imitation learning (IL) [6] and reinforcement learning (RL) [7]. For IL, suppose that the trajectories from the expert demonstration are close to optimal, IL can effectively learn to approximate the expert driving policy by reproducing expert actions given states, which could guarantee a lower bound of performance. For RL, the agent interacts with the environment and aims to optimize long-term reward and make better decisions using its collected experiences.

However, both these two paradigms have their own disadvantages. For IL, its ability is limited since its performance can at best amount to expert demonstrations. Besides, IL can easily encounter the distributional shift problem [8] because it only relies on static datasets. For RL, results from existing works indicate that its performance in urban scenarios is not satisfactory, probably because it only relies on reward signals, while in complex driving situations, the reward is sparse and hard to specify. Moreover, RL training consumes a huge amount of data and time. In order to mitigate the problems in both RL and IL and facilitate the development of the learning-based motion control strategy, a method that integrates reinforcement learning and learning from demonstrations should be considered. Combining the merits from RL with ones from IL, reinforcement learning from demonstration (RLfD) [9] is expected to not only accelerate the initial learning process of RL with the help of expert data, but also gain the potential of surpassing the performance of experts.

In this paper, we propose a novel framework combining reinforcement learning and expert demonstration to learn a motion control strategy for urban scenarios. The experiments are carried out in a roundabout scenario in the high-fidelity CARLA driving simulator. To reduce the complexity, we decompose the motion control of the vehicle into lateral control governed by a PID controller for path tracking and longitudinal control enabled by the proposed learning framework. We first collect human driving data as the expert demonstration dataset and then utilize the designed framework, which samples the experiences from both the expert demonstrations and the

agent’s self-exploration, to learn a motion control strategy. The results reveal that the proposed framework can effectively accelerate the learning process and accomplish better performance. The contributions of this paper are listed as follows.

- 1) An soft-actor-critic-based reinforcement learning from demonstration method is proposed, in which the learning process of the policy network is modified to accordingly combine maximizing the Q-function and imitating the expert demonstration.
- 2) A dynamic experience replay is proposed to adaptively adjust the sampling ratio between the agent’s self-exploration and the expert’s demonstration in the learning process.
- 3) A comprehensive test is carried out in a simulated urban driving scenario, where various RL and IL baselines are compared against our proposed method.

## II. RELATED WORK

### A. Deep reinforcement learning

Significant progress in deep reinforcement learning (DRL) has been made in recent years, expanding its applications in a wide variety of domains, especially in the field of robotics. Previous works have shown that the model-free DRL-based approach is promising for applications in autonomous learning motion control strategies, and thus much effort has been put on DRL-based methods. Zhang *et al.* implemented a vehicle speed control strategy using the double deep Q-network (DDQN) that utilizes visual representation as system input [10]. Chen *et al.* investigated four model-free DRL algorithms for motion control in a roundabout scenario, namely DDQN, deep deterministic policy gradient (DDPG), twin delayed DDPG (TD3), and soft actor-critic (SAC) [7], and the results demonstrated that the SAC algorithm outperforms the others. DRL has also been applied in dedicated motion control modules on the vehicle, which delivers favorable and robust performance. Chae *et al.* adopted DQN with a carefully-designed reward function for an adaptive braking system, which could effectively avoid collisions [11]. Ure *et al.* and Chen *et al.* successfully introduced DRL to tune the parameters in MPC [12] and PID [13] controllers, in order to achieve better and more stable performance in path tracking. Some of these DRL algorithms will be used as the baselines to show the effectiveness of our proposed method.

### B. Imitation learning

In addition to the DRL method, a renewed interest in imitation learning (IL) for autonomous driving has been raised. The behavior cloning method has become the prevailing method in end-to-end autonomous driving thanks to the significant improvement brought by deep neural networks. Xu. *et al.* proposed a combination of the fully convolutional network (FCN) and long-short term memory (LSTM) network for learning driving policy [14]. Codevilla *et al.* designed a conditional imitation learning framework which incorporates navigational command inputs [15]. Huang *et al.* presented a multimodal sensor fusion-based end-to-end driving system with imitation

learning and scene understanding [16]. Besides, some more sophisticated imitation learning methods have been proposed recently, including generative adversarial imitation learning (GAIL) [17], and Soft-Q imitation learning (SQIL) [18], in order to enable the agent to learn from demonstrations in a more effective way. These methods are used as the imitation learning baselines in the experiment.

### C. Reinforcement learning from demonstrations

Both RL and IL have inherent downsides, as stated in Section I, which gives rise to the concept of combining RL with IL for a more efficient learning process, i.e., reinforcement learning from demonstrations (RLfD). For example, Liu *et al.* [19] utilized DDPG with expert demonstration data in track following in The Open Racing Car Simulator (TORCS). Liang *et al.* brought forward controllable imitative reinforcement learning (CIRL) built upon DDPG and imitation learning for urban navigation [20]. Deep imitative model [21] proposed by Rhinehart *et al.* combined R2P2 and imitation learning to improve goal-directed planning. Our method is closely related to deep Q-learning from demonstrations (DQfD) [9] and DDPG from demonstrations (DDPGfD) [22], which incorporate small sets of expert demonstration data into experience replay and thus show a massively accelerated training process and better performance. However, our proposed method is based on SAC, which employs a maximum entropy and probabilistic setting rather than a deterministic manner (DDPG-based method). Besides, an adaptive experience sampling method is proposed to dynamically adjust the learning objectives.

## III. INTEGRATED REINFORCEMENT LEARNING AND IMITATION LEARNING FOR MOTION CONTROL

### A. Learning framework

As shown in Fig. 1, the learning framework is composed of three main parts. The simulated driving environment receives the actions of the agent or human expert and then emits the states of the environment. A human expert drives in the same environment using the steering wheel and pedals and their actions are collected in the demonstration dataset. For the RL driving agent, its motion control strategy is explicitly decomposed into longitudinal (acceleration) control with neural network (learnable) and lateral (steering) control with pure-pursuit and PID control (non-learnable) that tracks the predefined route. The learnable module can be trained with any IL or RL algorithms using expert demonstrations or specific rewards, and we train it using the proposed learning framework combining those two together, which is illustrated below.

The learning process follows the discrete-time Markov decision process (MDP). At every timestep  $t$ , the agent receives the state  $s_t$  of the environment and executes an action  $a_t$  according to its policy  $\pi(a_t|s_t)$ , and the environment returns a reward  $r_t$  and transitions to the next state  $s_{t+1}$ . The goal of RL is to optimize the policy to maximize the long-term expected returns (Q value):  $\max Q_\pi(s, a) = \max \mathbb{E}_\pi [\sum_t \gamma^t r(s_t, a_t)]$ . On the other hand, the goal is IL is to imitate the expert demonstrations, which can be represented as minimizing the

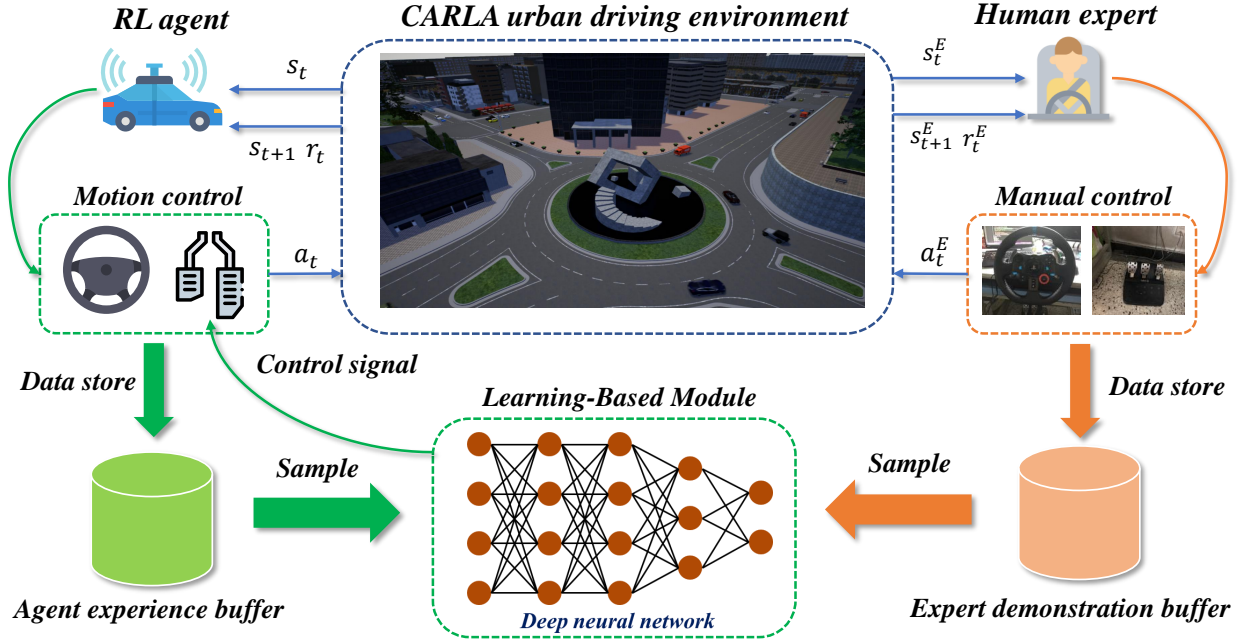


Fig. 1. An overview of our motion control system. The learnable module (deep policy network) receives bird-eye observations and generates throttle command. The lateral motion controller generates the steering command adaptively according to the throttle, predefined route, and vehicle states.

discrepancy (L2 norm) between the policy's action and the expert's action:  $\min \mathbb{E}_{\pi} \|\pi(a|s^E) - a^E\|_2$ . The core idea of our proposed approach is to add the IL target when using RL to train the motion control policy, in order to accelerate the training process and achieve better performance.

Therefore, as shown in Fig. 2, we maintain two experience replay buffers to store the agent's self-exploration experiences  $\mathcal{D}^S$  and expert demonstrations  $\mathcal{D}^E$  separately. The expert demonstrations in the buffer  $\mathcal{D}^E$  are in the format of state-action pairs along with the reward and state transition,  $\mathcal{D}^E : \{(s_t, a_t, r(s_t, a_t), s_{t+1})^E\}$ . In the training process, the policy  $\pi_{\phi}$  parameterized by  $\phi$ , samples a batch of mixed experiences from those two buffers with an adaptive ratio at each gradient update step. An off-policy DRL (SAC) learner integrated with imitation learning is introduced to carry out the training and the details of the learning process are given in the following subsections.

### B. Soft actor-critic with imitation learning

We implement the SAC algorithm with automatic entropy adjustment [23], augmented by the proposed experience replay mechanism and imitation learning objective, to train the policy network. SAC optimizes a stochastic policy in an off-policy manner and combines the actor-critic framework with the maximum entropy principle, which helps mitigate the issues on exploration-exploitation. The algorithm concurrently learns a policy network  $\pi_{\phi}$ , two Q-function networks  $Q_{\theta_1}, Q_{\theta_2}$ , and a value function network  $V_{\psi}$ . The Q-function networks are updated according to the following loss function:

$$\mathcal{L}(\theta_i) = \mathbb{E}_{(s_t, a_t, r_t, s_{t+1}) \sim \mathcal{D}} [(Q_{\theta_i}(s_t, a_t) - y_Q)^2], \quad (1)$$

where  $i = 1, 2$  and  $\mathcal{D}$  is composed of the experience collected by both the agent's self-exploration and the expert's demonstration  $\mathcal{D} = \mathcal{D}^E \cup \mathcal{D}^S$ . The target  $y_Q$  for Q-function update is given by:

$$y_Q = r(s_t, a_t) + \gamma V_{\text{target}}(s_{t+1}), \quad (2)$$

where  $V_{\text{target}}$  is the target value function network, which is obtained by Polyak averaging the value network  $V_{\psi}$  parameters at each gradient step.

The value function network  $V_{\psi}$  gets update through the following loss function:

$$\mathcal{L}(\psi) = \mathbb{E}_{s_t \sim \mathcal{D}} [(V_{\psi}(s_t) - y_V)^2], \quad (3)$$

and the target for value function is given by:

$$y_V = \min_{i=1,2} Q_{\theta_i}(s_t, \tilde{a}_t) - \alpha \log \pi_{\phi}(\tilde{a}_t | s_t), \quad (4)$$

where  $\alpha$  is a non-negative temperature parameter that controls the trade-off of the entropy term. The parameter is automatically tuned over the course of training according to [23]. The actions are obtained from the current policy  $\tilde{a}_t \sim \pi_{\phi}(\cdot | s_t)$ , where the states are sampled from the replay buffer  $s_t \sim \mathcal{D}$ .

The agent explores the environment according to its stochastic policy, i.e.,  $a_t \sim \pi_{\phi}(\cdot | s_t)$ , and the exploitation and exploration trade-off is controlled by the entropy of the policy, e.g., increasing entropy results in more exploration. In practice, we use the Gaussian policy and thus the policy network outputs two values that represent the mean and standard deviation of a Gaussian distribution, i.e.,  $a_t \sim \mathcal{N}(\mu_{\phi}(s_t), \sigma_{\phi}(s_t))$ . To make the stochastic policy differentiable, we use the reparameterization trick, in which a sample of actions from

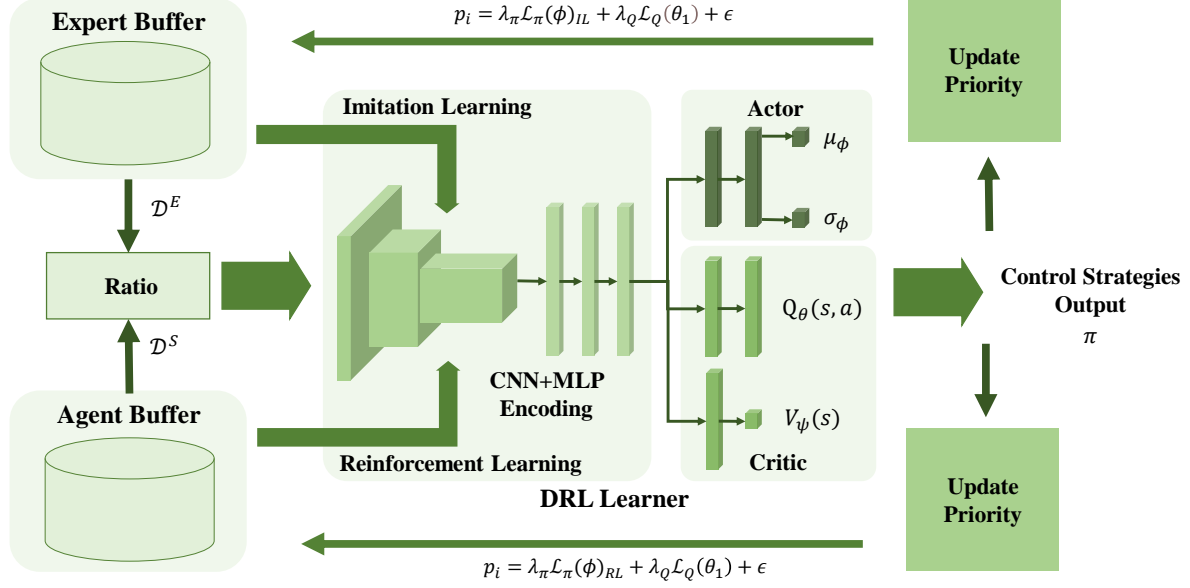


Fig. 2. The diagram of the proposed learning framework combining reinforcement learning and imitation learning. Batched transition tuple data from the agent and expert replay buffers is sampled at each gradient step to perform both reinforcement learning and imitation learning for learning driving policy.

the stochastic policy is drawn by computing the following deterministic function:

$$\tilde{a}_\phi(s_t) = \tanh(\mu_\phi(s_t) + \sigma_\phi(s_t) \odot \xi), \quad \xi \sim \mathcal{N}(0, I), \quad (5)$$

where  $\xi$  is independent Gaussian noise and  $\tanh$  is used to ensure that actions are bounded to a finite range.

We can utilize both imitation learning and reinforcement learning to optimize the policy network, leveraging the experiences from the expert demonstration and the agent's exploration, respectively. For reinforcement learning, the policy network should be updated to maximize the expected future return plus expected future entropy. The loss function for the policy network  $\pi_\phi$  when learning from the agent's experience should be:

$$\begin{aligned} \mathcal{L}(\phi)_{RL} = & \mathbb{E}_{s_t \sim \mathcal{D}^S} [\alpha \log \pi_\phi(\tilde{a}_\phi(s_t) | s_t) \\ & - \min_{i=1,2} Q_{\theta_i}(s_t, \tilde{a}_\phi(s_t))]. \end{aligned} \quad (6)$$

For learning from expert demonstrations or imitation learning, the loss function for updating the policy network  $\pi_\phi$  becomes:

$$\mathcal{L}(\phi)_{IL} = \mathbb{E}_{(s_t, a_t) \sim \mathcal{D}^E} [(\tilde{a}_\phi(s_t) - a_t)^2], \quad (7)$$

where  $\mathcal{D}^E$  is the buffer that contains expert demonstrations.

In the imitation loss function Eq. (7), the agent's action  $\tilde{a}_\phi(s_t)$  is the mean value of the stochastic policy  $\tanh(\mu_\phi(s_t))$ , instead of a sample from the action distribution. In addition, we add a Q-value regularization so as to combat the overfitting issue and boost the learning speed, which means

the imitation loss is only referred to if the following condition is satisfied:

$$Q_{\theta_j}(s_t^E, a_t^E) \geq \min_{i=1,2} Q_{\theta_i}(s_t^E, \tilde{a}_\phi(s_t^E)), \quad (8)$$

where  $j = 1, 2$ , meaning any of the two Q-function networks can trigger the condition.

Eq. (8) illustrates that the policy network will cease imitation loss update when the agent's performance (Q-value) outweighs the expert. Empirically speaking, adding this constraint can effectively adjust the imitation learning process and filter the suboptimal demonstrations, and avoid overfitting the policy to expert demonstrations.

Putting all together, the loss function for the policy network  $\pi_\phi$  in SAC with imitation learning is:

$$\mathcal{L}(\phi) = \begin{cases} \mathcal{L}(\phi)_{RL}, & \text{if } s_t \sim \mathcal{D}^S, \\ \mathcal{L}(\phi)_{IL}, & \text{if } (s_t, a_t) \sim \mathcal{D}^E \text{ and Eq. (8)}. \end{cases} \quad (9)$$

To balance the sources of experience the agent learns from (i.e., the ratio of the agent's experience and expert's demonstration), we design a mechanism of experience replay that can adaptively sample experiences from the two sources, which is explained below.

### C. Adaptive prioritized experience replay

Following the prioritized experience replay (PER) mechanism [24], each transition tuple in the two replay buffers will be assigned a priority, such that more important transition tuples with greater approximation errors can more likely be

sampled. This way, the sampling process becomes more efficient and goal-directed. The devised priority  $p_i$  for transition tuple  $i$  in the agent replay buffer is:

$$p_i^{RL} = \lambda_\pi \mathcal{L}_\pi(\phi)_{RL} + \lambda_Q \mathcal{L}_Q(\theta_1) + \epsilon, \quad (10)$$

where  $\lambda_\pi$  and  $\lambda_Q$  are the weights to balance the importance of each error term, and  $\epsilon$  is a small positive constant to ensure that all transitions are sampled with some non-zero probability. Likewise, the priority  $p_i$  for transition tuple  $i$  in the expert replay buffer is

$$p_i^{IL} = \lambda_\pi \mathcal{L}_\pi(\phi)_{IL} + \lambda_Q \mathcal{L}_Q(\theta_1) + \epsilon. \quad (11)$$

The probability for a transition tuple being sampled is  $P(i) = \frac{p_i^\omega}{\sum_k p_k^\omega}$ , in which  $\omega$  is a hyper-parameter that determines the level of prioritization. To correct the bias introduced by not uniformly sampling during backpropagation, an importance-sampling weight is assigned to the loss regarding the transition tuple  $w(i) = (\frac{1}{NP(i)})^\beta$ , where  $N$  is the number of experience tuples in the buffer and  $\beta$  is another hyper-parameter that controls how much prioritization to apply.

We sample the experiences separately for expert and agent buffers while updating the priorities of them, and the ratio of the samples from the two sources is dynamically adjusted using the following equation:

$$\mathcal{B} \leftarrow (\rho \mathcal{B} \sim \mathcal{D}^S) \cup ((1 - \rho) \mathcal{B} \sim \mathcal{D}^E), \quad (12)$$

where  $\mathcal{B}$  is a mini-batch, and  $\rho \in [0, 1]$  is the sampling ratio, which is updated after an episode is done according to:

$$\rho \leftarrow \rho + \frac{1}{N_B} \mathbb{1} \left( \sum_t r_t^A \geq \bar{r}^E \right), \quad (13)$$

where  $N_B$  is the size of the mini-batch,  $\sum_t r_t^A$  denotes the episodic reward of the agent, and  $\bar{r}^E$  represents the average episodic reward of the expert demonstration. It indicates that the sampling ratio for the agent buffer will gradually increase if the episodic reward for the agent is greater than the average performance of the expert. For a more specific illustration of the learning framework, the pseudo-code implementation is given in Algorithm 1.

#### IV. EXPERIMENTS

##### A. Experimental Setup

We employ the CARLA simulator [25] as the experimental platform, since it possesses abundant vehicle models and maps close to the real world, thus being suitable for urban driving simulation. The autonomous vehicle is tasked to run safely and time-efficiently through a roundabout consisting of multiple intersections in the urban area, shown in Fig. 3(a). The starting and destination areas are fixed but the traffic flows vary in different training episodes. The ego vehicle is first spawned randomly within the starting area and follows the planned route to the destination, while avoiding collisions with the surrounding vehicles in the dense traffic. We only consider surrounding vehicles, including motorcycles, sedans, and trucks, as traffic participants and a total of 100 vehicles are

#### Algorithm 1 Soft Actor-Critic with Imitation Learning

---

**Input:** Expert demonstration buffer  $\mathcal{D}^E$ , initial sampling ratio  $\rho$ , initial entropy parameter  $\alpha$ , Polyak averaging weight  $\lambda$ .

- 1: Initialize policy network  $\phi$ , value network  $\psi$ , and Q networks  $\theta_i, i = 1, 2$
- 2: Initialize target value network  $V_{target} \leftarrow V_\psi$
- 3: Initialize empty agent replay buffer  $\mathcal{D}^S$
- 4: **repeat**
- 5:   Observe state  $s_t$  and sample action  $a_t \sim \pi_\phi(\cdot|s_t)$
- 6:   Execute the action  $a_t$  in the environment
- 7:   Observe the next state  $s_{t+1}$  and reward  $r_t$
- 8:   Store the transition  $(s_t, a_t, r_t, s_{t+1})$  in agent buffer  $\mathcal{D}^S$
- 9:   **if** time to update **then**
- 10:     Sample a mini-batch  $\mathcal{B} \sim (\mathcal{D}; \mathcal{D}^E)$  using Eq.(12)
- 11:     Update Q networks  $\theta_i$  using Eq.(1) and Eq.(2)
- 12:     Update value network  $\psi$  using Eq.(3) and Eq.(4)
- 13:     Update target value networks  $V_{target}$ :
- 14:      $V_{target} \leftarrow \lambda \psi + (1 - \lambda) V_{target}$
- 15:     Update policy network  $\phi$  using Eq.(9)
- 16:     Update entropy parameter  $\alpha$
- 17:     Update priorities of transition tuples  $p_i^{RL}$  and  $p_i^{IL}$  using Eq.(10) and Eq.(11) respectively
- 18:   **end if**
- 19:   **if**  $s_{t+1}$  is terminal **then**
- 20:     Reset environment state
- 21:     Update sampling ratio  $\rho$  using Eq.(13)
- 22:   **end if**
- 23: **until** Convergence

---

randomly spawned in the scene. Each of them is assigned with a random route by the built-in route planner in the CARLA simulator using the A\* algorithm given the random start point and destination. The surrounding vehicles are running by keeping the target speed (8 m/s) and performing emergency stop when detecting potential danger to the nearby vehicles. Note that although the behaviors of surrounding vehicles are the same, the number of vehicles in the roundabout area and their routes are varied in different episodes, and thus the traffic situations the agent vehicle faces are highly stochastic. The simulation timestep is 0.1 seconds and a training episode ends when encountering the following cases: 1) the ego vehicle reaches the destination area; 2) the ego vehicle collides with other vehicles; 3) the episode exceeds the maximum time steps (800).

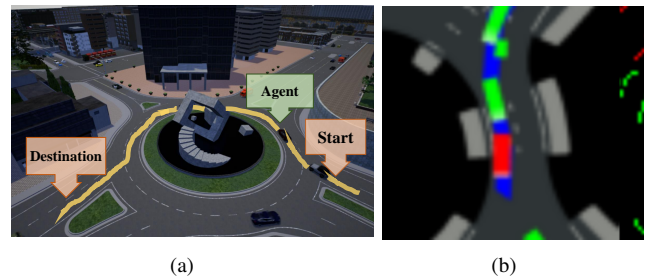


Fig. 3. Overview of the urban driving task and processed scene representation: (a) overview of the roundabout; (b) an example of bird-view image input.

We take the bird-eye view image shown in Fig. 3(b) as the scene representation because it contains rich information of the ego vehicle and its route, the road topology, and surrounding vehicles. The bird-eye view image can be obtained from the upstream perception module that can process the information from the sensor system, localization system, and high-definition map. Since this work focuses on the decision-making process, we assume that the perception information is perfect and ignore the problem of perception uncertainty, which means the states of the ego vehicle and all surrounding objects, as well as other information on the road, can be projected into a bird-eye view map accurately. The bird-eye view image is an RGB image encoding different information about the driving environment. The drivable areas and lane markings are rendered in grey and white, and the planned route for the ego vehicle is rendered as a thick blue polyline. The historical bounding box of the ego vehicle is rendered in red while the historical bounding boxes of the detected surrounding vehicles are rendered as green boxes. The image is with a pixel size of  $64 \times 64 \times 3$ , encoding a field of view with a size of  $40 \times 40 \text{ m}^2$ . The image is aligned to the ego vehicle's local coordinate where the ego vehicle is positioned at the center.

We decouple the vehicle motion control into longitudinal and lateral directions. Considering that the vehicle basically just needs to follow the drive lane in the lateral direction, to reduce the complexity of the problem and guarantee lateral control stability, the lateral control (steering) is conducted by a pure-pursuit controller to track the target waypoint on the planned route. For the longitudinal control, we utilize two kinds of action spaces for different algorithms. The continuous action space is the normalized throttle and brake control  $[-1, 1]$ , where  $[-1, 0]$  is for brake input and  $[0, 1]$  for throttle input, and the discrete action space consists of three actions corresponding to the normalized throttle and brake, which are  $\{-1, 0, 1\}$ . The policy network employs the convolutional neural network (CNN) structure as the feature extractor and generates the mean and standard deviation of a Gaussian distribution through two fully connected layers, each with 64 hidden units. The critic networks' feature extractors share the same CNN structure.

In the stage of collecting expert demonstration data, a human expert with a driving license is asked to demonstrate his execution to finish the driving task in the CARLA environment. The expert observes the driving environment from a front-view camera on the vehicle with the instant speed information displayed at the same time, and controls the pedal of a Logitech G29 driving set to output continuous actions or presses the keyboard to output discrete maneuvers. It is worth noting that the expertise of the human participant is relative to the RL agent because humans possess prior knowledge on scene understanding and driving with the common goal to drive safely and efficiently. Therefore, the human expert is just asked to drive as usual to finish the task without imposing any other requirements but the speed limit. Overall, a total of 50 trajectories of expert demonstrations are collected

for continuous actions, with approximately 15,000 transition tuples. The same amount of trajectories are also collected for discrete maneuvers.

### B. Reward function

Considering that safety is the most critical in autonomous driving, we design a reward function that focuses on safety factors while keeping a balance on efficiency and ride comfort. After some trials, the reward function is designed as a combination of four features:

$$r_t = r_v + 0.1r_{step} + 10r_{col} + 0.8r_{safe}. \quad (14)$$

The first term  $r_v$  is for travel efficiency, which stimulates the agent to run as fast as possible but within the speed limit  $v_{max}$ :

$$r_v = v + 2(v_{max} - v) \mathbb{1}(v \geq v_{max}), \quad (15)$$

where  $v$  is the speed of the ego vehicle.

The second term  $r_{step} = -1$  is a constant step penalty and devised to encourage the agent to complete the task as quickly as possible.

The other two terms are set for ensuring safety. First of all,  $r_{col} = -1$  is a penalty for collision. However, only giving the collision signal might be too weak and lead to spurious correlations between some irrelevant features and actions. Therefore, to provide more information to the reward signal, we consider the potential danger in the front-detection zone shown in Fig. 4. It consists of two fan-shape areas  $Z_1(\alpha_1, r_1)$  and  $Z_2(\alpha_2, r_2)$ , where  $\alpha_i$  is the detect angle and  $r_i$  is the radius.  $Z_2$  is a long-range detection area originating from the vehicle center  $(x_A, y_A)$  for tasks such as car following.  $Z_1$ , centered at the front of the vehicle  $(x_A + \frac{L_{wb}}{2}, y_A)$  where  $L_{wb}$  is the length of the wheelbase, is responsible for short distance sensing like a car passing by in front of ego vehicle. If multiple vehicles are in an area  $Z_i$ , only the nearest vehicle is detected and its distance to a certain center point  $d_i$  will be returned. Utilizing the information above, we can derive the safety reward  $r_{safe}$  as:

$$r_{safe} = - \left[ \lambda_s \frac{r_1 - d_1}{r_1} \mathbb{1}(d_1) + (1 - \lambda_s) \frac{r_2 - d_2}{r_2} \mathbb{1}(d_2) \right] v_{safe}, \quad (16)$$

where  $\lambda_s = 0.8$  is a weight balancing the importance of the two areas,  $d_i$  is the distance of the ego vehicle to the nearest vehicle in each area  $Z_i$ , and  $v_{safe}$  is a speed-related regulator:

$$v_{safe} = v [1 - \mathbb{1}(v \leq v_{min}, a_t \leq 0)], \quad (17)$$

where  $v_{min}$  is a speed threshold and  $a_t$  is the agent's action.

Eq. (16) directs the ego vehicle to avoid collisions, since the normalized term will be close to 1 if two vehicles are too close, and thus the penalty will increase. If there is no vehicle in the detection zone, the normalized term will be 0 due to the indicator term, and no penalty is given. We also add a regulator (Eq. (17)) to the safety penalty, which increases the penalty if the ego vehicle is running fast when there is a potential danger in the front zone and removes the penalty if the ego vehicle decelerates or waits when facing traffic congestion.



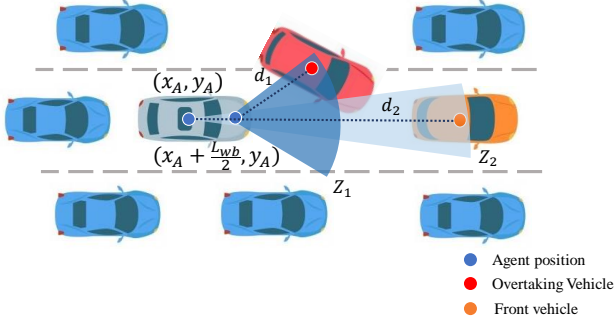


Fig. 4. Illustration of the front-detection area for the ego vehicle.

### C. Comparison baselines

To make a comprehensive evaluation of the performance of the proposed approach, we compare it with other existing methods from the field of DRL, IL, and RLfD. The baseline DRL algorithms are:

- 1) **DQN** [26]: one of the first and most-commonly known DRL methods. It is a value-based method and Q-function loss gets update through one-step temporal difference error.
- 2) **PPO** [27]: an on-policy method and has been widely used in robotics control.
- 3) **TD3** [28]: an improved method with twin delayed Q-networks based on the DDPG algorithm.
- 4) **A3C** [29]: an on-policy actor-critic framework with asynchronous sampling and advantage estimation.
- 5) **SAC** [30]: the basis of our approach, which has been recently reported with higher performance in practical applications.

The imitation learning baseline methods are listed as follows:

- 1) **BC**: behavioral cloning is a supervised learning method, which has been commonly used in learning driving policy from expert demonstrations.
- 2) **SQIL** [18]: a regularized behavioral cloning method, which combines the maximum likelihood of BC with regularization that can stimulate the agent return to demonstrated states upon encountering new states.
- 3) **GAIL** [31]: a variant of imitation learning using generative adversarial training, in which the generator is RL-based and the reward function comes from the discriminator that tries to tell apart the demonstrated and generated trajectories.

Moreover, we take **DQfD** [9] as the reinforcement learning from demonstration baseline method. The DQN, DQfD, and SQIL baseline methods are implemented with discrete action space, and the rest of the baseline methods (PPO, TD3, SAC, A3C, BC, GAIL, and our proposed approach) are implemented with continuous action space.

### D. Implementation details

Our proposed approach and other baseline methods are trained for 100k steps. The neural networks are trained on a single NVIDIA RTX 2070 Super GPU using Tensorflow and Adam optimizer with a learning rate of  $3 \times 10^{-4}$ , and

the training process takes roughly 6 hours. The parameters related to the experiment are listed in Table I. All the listed algorithms are trained once with the same total training steps, and the policy networks are saved after finishing an episode during training. For each algorithm, we take the trained policy network with the highest episodic return for the subsequent testing phase.

TABLE I  
PARAMETERS USED IN THE EXPERIMENT

Notation	Meaning	Value
$v_{max}$	Speed limit (m/s)	12
$v_{min}$	Speed threshold (m/s)	0.1
$\alpha_{i=1,2}$	Angles of front detection area (deg)	60, 30
$r_{i=1,2}$	Radius of front detection area (m)	10, 20
$L_{wb}$	Wheelbase (mm)	2850
$\gamma$	Discount rate	0.995
$\lambda$	Polyak averaging weight	0.005
$\alpha$	Initial entropy weight	1
$\mathcal{H}_{min}$	Desired minimum expected entropy	-1
$N_{buffer}$	Agent buffer capacity	50000
$N_B$	Mini-batch size	64
$\rho$	Initial sampling ratio	0.3
$\omega$	Hyperparameter for PER	0.6
$\beta$	Hyperparameter for PER	0.4
$\epsilon$	Hyperparameter for PER	$10^{-6}$
$\lambda_\pi$	Priority balance weight	1
$\lambda_Q$	Priority balance weight	1

## V. RESULTS AND DISCUSSIONS

### A. Training results

We evaluate the training performance of our proposed method in comparison with other RL and IL methods introduced in the previous section. Fig. 5 shows the training result of each RL baseline algorithm for 100k training steps, and the black dotted line represents an average episode reward (940.81) that an agent can get reaching the destination area. Fig. 6 shows the training result of the IL algorithms, and the grey shade area in Fig. 6 is the performance of the expert demonstrations with a mean episode reward of 1060.4 (dash-dotted line) and standard deviation of 227.0.

As seen in Fig. 5, compared with other RL baseline methods, our proposed method shows a faster convergence speed and better performance at the end. We can find out that the average episodic reward of the proposed method quickly climbs to a very high level and gradually improves and finally converges after roughly 40k steps. At the beginning of the training process, with a larger part of samples from expert demonstration, the agent is basically imitating the expert demonstration with high rewards. Then, with the training going on and the agent's performance getting better, more experience from the agent's self-exploration will be sampled, and thus the training process leans towards reinforcement learning. For the on-policy methods, A3C behaves poorly and can barely reach the entrance of the roundabout. It is because the traffic scenario for each training epoch is notably different, and the A3C policy easily falls into a local minimum of staying close to the starting point. PPO can mitigate this

problem to some extent and quickly learn to move forward in the first few episodes, thereby gaining a relatively higher reward at the beginning, but it still cannot learn to reach the destination with dense traffic, showing a limited performance. The three off-policy algorithms perform well and they all can basically reach the destination. SAC performs the best but takes longer steps to converge. DQN actually performs well with only discrete action space due to using double Q-networks, dueling branch, and PER. This is because the value-based method can at least guarantee the training progress, but is heavily relied on the design of the reward function. TD3 takes the longest steps to actually improve the policy, and is very unstable in performance during our experiment: it shows no progress without adding noise, but after adding the noise, its performance still varies greatly. As a closely related method to ours, the DQfD algorithm shows a faster adaptation efficiency and its reward curve converges faster. However, the final performance of DQfD is pretty close to the DQN method and lower than SAC and our proposed method. This is because the policy update of DQfD only depends on the Q values from the Q-network and thus expert demonstrations are not fully exploited, whereas our proposed approach also utilizes expert demonstrations for policy updates. Therefore, the performance of the DQfD baseline cannot reach the same level as our proposed approach.

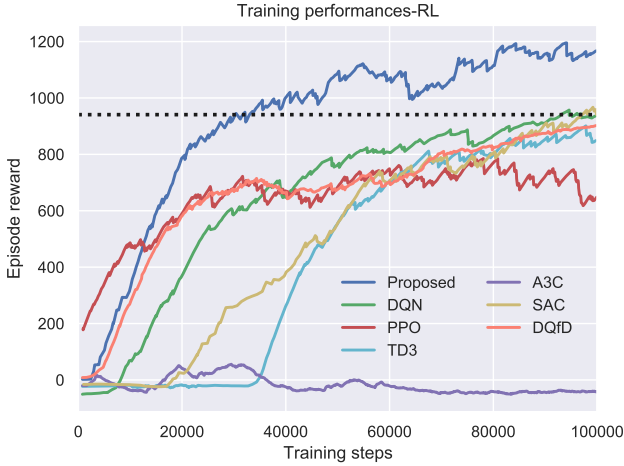


Fig. 5. The training curves of RL baselines and our approach. Our approach shows the highest episode reward than other methods at the end of training.

In comparison with other IL baseline methods, our approach converges quite fast and quickly reaches the level of the human expert. SQIL can also converge very fast but performs notably worse than our method in terms of average episodic reward as it only uses expert demonstration data. GAIL shows the worst performance, probably because it is good at deal with low-dimensional state inputs but fails to handle high-dimensional image inputs, which has also been mentioned by [8] and [18]. The results reveal that our approach can not only imitate the expert demonstrations but also improve the performance to some extent because of adding RL to

the framework. For the behavior cloning method, because its learning mechanism is different from other methods (only offline supervised learning), we only show its testing results in the next subsection.

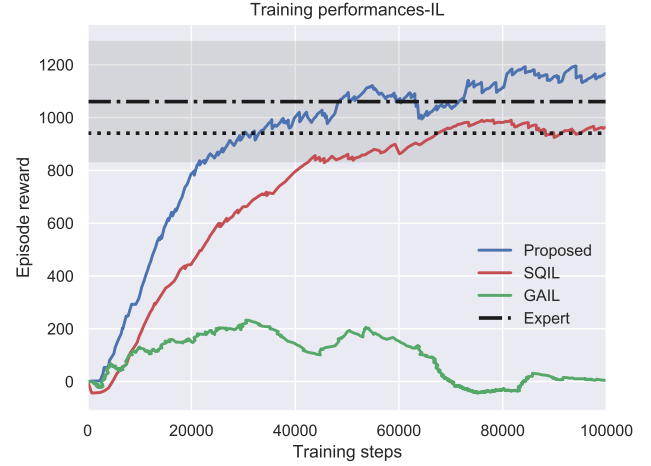


Fig. 6. The training curves of IL baselines and our approach. Our approach shows a faster convergence as well as steady progress.

Wrapping up, the performance improvement of our proposed method may come from three factors. First of all, the off-policy RL setting ensures that more abundant and diverse trajectories are stored in the buffer, and the dynamic PER we introduced can make sure that these stored agent trajectories and the expert trajectories can be reused efficiently. Furthermore, we adopt the SAC algorithm that optimizes a stochastic policy through entropy regularization, which brings better exploration capability. Eventually, the introduction of expert demonstration trajectories and imitation learning objectives into the policy training guarantees a lower bound of agent performance, as well as making a faster adaptation for convergence, which is why our proposed method outcompetes other off-policy methods including SAC.

## B. Testing results

The testing scenario is the same as the training scenario in the roundabout but with different traffic conditions. The surrounding traffic participants are randomly spawned in the scene, and each is assigned with a random route in every epoch. We use the trained policy for each method to control the vehicle to navigate through the roundabout. The success rate, collision rate, average episodic reward, and episodic length are recorded and the summary of test performance of all the methods is given in Table II. The results reflect that our proposed approach achieves a high success rate, as well as reaching the destination in a shorter time. In line with the training results, A3C does not perform well, and the BC method also suffers from a low success rate due to the distributional shift during the test. SAC and DQN show good performance during the test, and SQIL is also quite effective in solving this problem.



TABLE II  
SUMMARY OF THE TEST RESULTS

Method	Success rate (%)	Collision rate (%)	Episode reward	Episode length (s)
BC	16	52	987.37 $\pm$ 248.60	48.7 $\pm$ 10.4
A3C	18	49	39.844 $\pm$ 42.764	49.3 $\pm$ 2.5
Rule-based	60	40	940.44 $\pm$ 337.21	<b>21.1</b> $\pm$ 5.0
GAIL	65	26	769.32 $\pm$ 235.47	24.5 $\pm$ 6.4
PPO	65	31	903.69 $\pm$ 253.74	32.1 $\pm$ 8.3
TD3	67	29	802.45 $\pm$ 184.66	31.6 $\pm$ 5.9
SAC	76	14	1050.9 $\pm$ 205.80	41.0 $\pm$ 8.4
SQIL	78	12	966.35 $\pm$ 199.13	38.2 $\pm$ 8.2
DQN	79	18	1006.3 $\pm$ 191.28	38.4 $\pm$ 8.4
DQfD	80	17	1092.6 $\pm$ 149.07	35.0 $\pm$ 7.2
Ours	90	8	1205.3 $\pm$ 135.79	23.9 $\pm$ 6.5
Ours+Safety	<b>93</b>	<b>5</b>	<b>1227.1</b> $\pm$ 124.05	22.8 $\pm$ 5.5

In addition, we add two rule-based methods as comparisons. The first method is a pure rule-based controller that follows the default rule defined by the CARLA simulator. The vehicle will follow the target speed by a PID controller, and will emergently stop if encountering obstacles in a fan shape area like  $Z_i$  in our reward design. The second one combines our RL-based controller with a rule-based safety controller that will take over the control (emergency brake) if encountering near-collision situations. The results in Table II indicate that pure ruled-based system does not perform very well. Although the rule-based controller can occasionally finish the task in a shorter time, it suffers from a lower success rate, mainly because of collision with other vehicles. This is because the rules are very simple and the vehicle cannot timely stop to avoid collision with other vehicles. On the other hand, combing RL and rule-based controllers are beneficial in the testing, leading to a higher success rate. When it comes to a real-world scenario, we can design more sophisticated rules to derive a safety control system and combine it with an RL-based control module to ensure both safety and efficiency.

Fig. 7 shows some of the trajectories given by our proposed motion control strategy, which demonstrate that the agent vehicle is able to cruise at a safe distance following the front vehicle. The success trajectory shows that the agent vehicle can go through the roundabout scene to the destination area with smooth turnings and decelerate gradually when facing stopped cars in the front. However, the faint yellow points indicate the failure cases, which are mostly owing to collisions with the front vehicle or overtaking vehicles from the side. The collisions that happened right into the roundabout mainly come from the vehicles from the left or right side since the blind angle for the detection area gets larger when going into the roundabout. Some failure cases at the very beginning are due to the control errors of the surrounding vehicles in the CARLA simulator, which could cause a collision with the ego vehicle.

To have a more intuitive sense of the safety and efficiency issues, we have a further look at the speed control performance of each method. In addition to the aforementioned approaches, we also randomly sampled 30 human driving trajectories in the expert dataset. Speed information in the initial 20 seconds from the beginning of an episode is calculated for each method. As shown in Fig. 8, the speed profile of our proposed method is very close to the performance of a human expert, which shows both quick responsiveness and steadiness. The DQfD

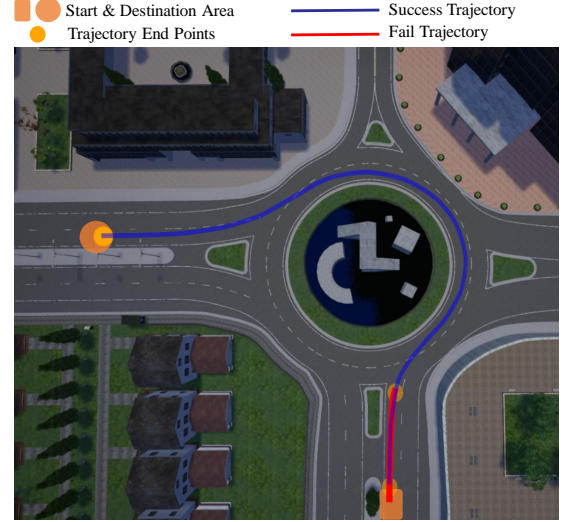


Fig. 7. An overview of vehicle trajectories of the proposed method during testing. The orange areas represent the starting and destination zones. The yellow points show where the trajectory end.

method has a similar performance but with a higher fluctuation in speed and the SQIL method has a better steadiness but lower speed. The TD3 algorithm reacts the fastest, but its speed varies greatly after the initial acceleration, which obviously cannot guarantee safety. Other RL agents accelerate steadily but are unable to reach a speed above 6 m/s in 20 seconds.

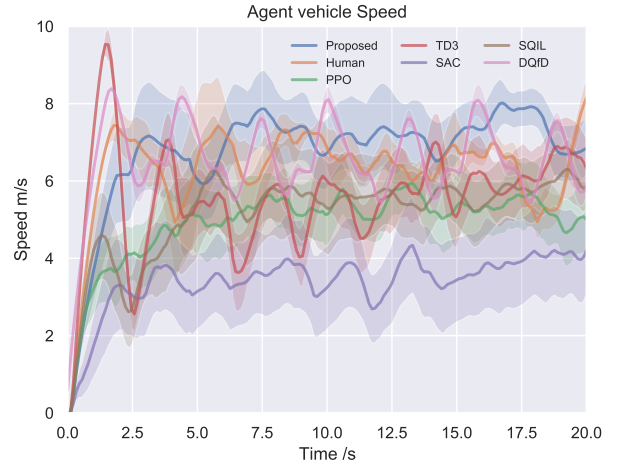


Fig. 8. The average speed and its standard deviation in the first 20 seconds after initial acceleration for each method

### C. Ablation study

To investigate the influence of different components of our proposed approach, we carry out an ablation study. Specifically, we remove the prioritized replay and Q-filter respectively, which are two major points of the proposed method, to investigate their effects on the training performance. The results in Fig. 9 manifest that without prioritized replay, the training performance drops throughout the training process. This shows that prioritized replay can effectively adjust the

training process by choosing more significant transitions so that learning becomes more efficient. Moreover, the Q-filter proposed in Eq. (8) and Eq. (9) has a more significant impact on the training performance because the Q-filter can discard some sub-optimal expert demonstration data from the sampled batch, and thus the agent is apt to learn actions that have a higher reward.

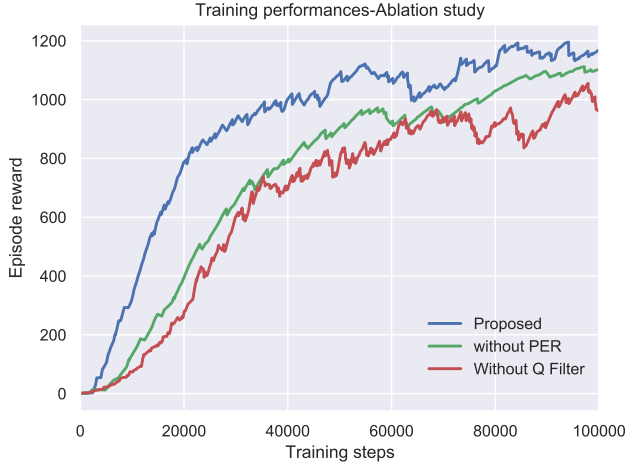


Fig. 9. The training curves for ablation study of our approach.

#### D. Discussions

Some limitations of this work should be acknowledged. First of all, the generalization capability of the proposed method needs further investigation. For now, we only validate the feasibility and improvement of our method in the roundabout scenario, but its generalization ability in other urban traffic scenarios such as left turns and intersections is not explored. Secondly, our method cannot guarantee a 100% safety rate, even if a rule-based safety controller has been added to the system. In safety-critical autonomous driving tasks, it is a must to further improve the safety performance of our method. Therefore, future work may fall in the following directions. First, we need to test the generalization capability under different urban traffic scenarios or even in a whole simulated city environment. Second, the safety of the system needs critical improvement. We can either improve the capacity and quality of expert demonstrations and refine the design of the reward function, or polishing the rule-based safety controller to take over the vehicle when the RL-based controller fails. Third, to further manifest the advantage of our method, we can compare it with more baseline methods, including human-guidance-based learning algorithms such as dataset aggregation (Dagger). Other practical issues such as how to project the raw sensory data to the birds-eye-view representation and handling the perception uncertainty that exists in the state input to the RL decision module are also worth exploration.

#### VI. CONCLUSIONS

In this paper, we propose a motion control strategy for urban autonomous driving, with an improved learning framework

that incorporates deep reinforcement learning and imitation learning from expert demonstrations. A novel reinforcement learning algorithm with expert demonstrations is put forward to leverage human prior knowledge, in order to improve the sample efficiency and performance. Specifically, we modify the update of the policy network by combining maximizing the Q-function and imitating the expert's actions, and design an adaptive experience replay method to adaptively sample experience from the agent's self-exploration and expert demonstration for policy update. We validate the proposed method in a simulated challenging urban roundabout scenario with dense traffic. A comprehensive comparison with other RL and IL baselines validates that our method has better sample efficiency and performance in the training process. The testing result reveals that our proposed method can achieve a higher success rate with less time to reach the destination. We also demonstrate that combining a rule-based safety controller with the RL-based controller can further improve the success rate. The ablation study shows that the two major components in our method, which are prioritized replay and expert demonstration filter, play important roles in improving the learning performance. The above results reflect the promising potential of our approach being applied in the autonomous vehicle motion control strategy.

#### REFERENCES

- [1] S. Panwai and H. Dia, "Comparative evaluation of microscopic car-following behavior," *IEEE Transactions on Intelligent Transportation Systems*, vol. 6, no. 3, pp. 314–325, 2005.
- [2] B. Paden, M. Čáp, S. Z. Yong, D. Yershov, and E. Frazzoli, "A survey of motion planning and control techniques for self-driving urban vehicles," *IEEE Transactions on intelligent vehicles*, vol. 1, no. 1, pp. 33–55, 2016.
- [3] S. Aradi, "Survey of deep reinforcement learning for motion planning of autonomous vehicles," *IEEE Transactions on Intelligent Transportation Systems*, 2020.
- [4] L. Chen *et al.*, "A reinforcement learning-based adaptive path tracking approach for autonomous driving," *IEEE Transactions on Vehicular Technology*, 2020.
- [5] S. Panwai and H. Dia, "Comparative evaluation of microscopic car-following behavior," *IEEE Transactions on Intelligent Transportation Systems*, vol. 6, no. 3, pp. 314–325, 2005.
- [6] A. O. Ly and M. A. Akhloufi, "Learning to drive by imitation: an overview of deep behavior cloning methods," *IEEE Transactions on Intelligent Vehicles*, 2020.
- [7] J. Chen, B. Yuan, and M. Tomizuka, "Model-free deep reinforcement learning for urban autonomous driving," in *2019 IEEE Intelligent Transportation Systems Conference (ITSC)*. IEEE, 2019, pp. 2765–2771.
- [8] K. Brantley, W. Sun, and M. Henaff, "Disagreement-regularized imitation learning," in *International Conference on Learning Representations*, 2019.
- [9] T. Hester, M. Vecerik, O. Pietquin, M. Lanctot, T. Schaul, B. Piot, D. Horgan, J. Quan, A. Sendonaris, I. Osband *et al.*, "Deep q-learning from demonstrations," in *Proceedings of the AAAI Conference on Artificial Intelligence*, vol. 32, no. 1, 2018.
- [10] Y. Zhang, P. Sun, Y. Yin, L. Lin, and X. Wang, "Human-like autonomous vehicle speed control by deep reinforcement learning with double q-learning," in *2018 IEEE Intelligent Vehicles Symposium (IV)*. IEEE, 2018, pp. 1251–1256.
- [11] H. Chae, C. M. Kang, B. Kim, J. Kim, C. C. Chung, and J. W. Choi, "Autonomous braking system via deep reinforcement learning," in *2017 IEEE 20th International Conference on Intelligent Transportation Systems (ITSC)*. IEEE, 2017, pp. 1–6.

- [12] N. K. Ure, M. U. Yavas, A. Alizadeh, and C. Kurtulus, "Enhancing situational awareness and performance of adaptive cruise control through model predictive control and deep reinforcement learning," in *2019 IEEE Intelligent Vehicles Symposium (IV)*. IEEE, 2019, pp. 626–631.
- [13] L. Chen, Y. Chen, X. Yao, Y. Shan, and L. Chen, "An adaptive path tracking controller based on reinforcement learning with urban driving application," in *2019 IEEE Intelligent Vehicles Symposium (IV)*. IEEE, 2019, pp. 2411–2416.
- [14] H. Xu, Y. Gao, F. Yu, and T. Darrell, "End-to-end learning of driving models from large-scale video datasets," in *Proceedings of the IEEE conference on computer vision and pattern recognition*, 2017, pp. 2174–2182.
- [15] F. Codevilla, M. Müller, A. López, V. Koltun, and A. Dosovitskiy, "End-to-end driving via conditional imitation learning," in *2018 IEEE International Conference on Robotics and Automation (ICRA)*. IEEE, 2018, pp. 1–9.
- [16] Z. Huang, C. Lv, Y. Xing, and J. Wu, "Multi-modal sensor fusion-based deep neural network for end-to-end autonomous driving with scene understanding," *IEEE Sensors Journal*, pp. 1–1, 2020.
- [17] A. Kuefler, J. Morton, T. Wheeler, and M. Kochenderfer, "Imitating driver behavior with generative adversarial networks," in *2017 IEEE Intelligent Vehicles Symposium (IV)*. IEEE, 2017, pp. 204–211.
- [18] S. Reddy, A. D. Dragan, and S. Levine, "Sqil: Imitation learning via reinforcement learning with sparse rewards," *arXiv preprint arXiv:1905.11108*, 2019.
- [19] K. Liu, Q. Wan, and Y. Li, "A deep reinforcement learning algorithm with expert demonstrations and supervised loss and its application in autonomous driving," in *2018 37th Chinese Control Conference (CCC)*. IEEE, 2018, pp. 2944–2949.
- [20] X. Liang, T. Wang, L. Yang, and E. Xing, "Cirl: Controllable imitative reinforcement learning for vision-based self-driving," in *Proceedings of the European Conference on Computer Vision (ECCV)*, 2018, pp. 584–599.
- [21] N. Rhinehart, R. McAllister, and S. Levine, "Deep imitative models for flexible inference, planning, and control," *arXiv preprint arXiv:1810.06544*, 2018.
- [22] M. Vecerik, T. Hester, J. Scholz, F. Wang, O. Pietquin, B. Piot, N. Heess, T. Rothörl, T. Lampe, and M. Riedmiller, "Leveraging demonstrations for deep reinforcement learning on robotics problems with sparse rewards," *arXiv preprint arXiv:1707.08817*, 2017.
- [23] T. Haarnoja, A. Zhou, K. Hartikainen, G. Tucker, S. Ha, J. Tan, V. Kumar, H. Zhu, A. Gupta, P. Abbeel *et al.*, "Soft actor-critic algorithms and applications," *arXiv preprint arXiv:1812.05905*, 2018.
- [24] T. Schaul, J. Quan, I. Antonoglou, and D. Silver, "Prioritized experience replay," *arXiv preprint arXiv:1511.05952*, 2015.
- [25] A. Dosovitskiy, G. Ros, F. Codevilla, A. Lopez, and V. Koltun, "Carla: An open urban driving simulator," *arXiv preprint arXiv:1711.03938*, 2017.
- [26] H. Van Hasselt, A. Guez, and D. Silver, "Deep reinforcement learning with double q-learning," *arXiv preprint arXiv:1509.06461*, 2015.
- [27] J. Schulman, F. Wolski, P. Dhariwal, A. Radford, and O. Klimov, "Proximal policy optimization algorithms," *arXiv preprint arXiv:1707.06347*, 2017.
- [28] S. Fujimoto, H. Van Hoof, and D. Meger, "Addressing function approximation error in actor-critic methods," *arXiv preprint arXiv:1802.09477*, 2018.
- [29] V. Mnih, A. P. Badia, M. Mirza, A. Graves, T. Lillicrap, T. Harley, D. Silver, and K. Kavukcuoglu, "Asynchronous methods for deep reinforcement learning," in *International conference on machine learning*, 2016, pp. 1928–1937.
- [30] T. Haarnoja, A. Zhou, P. Abbeel, and S. Levine, "Soft actor-critic: Off-policy maximum entropy deep reinforcement learning with a stochastic actor," *arXiv preprint arXiv:1801.01290*, 2018.
- [31] J. Ho and S. Ermon, "Generative adversarial imitation learning," in *Advances in neural information processing systems*, 2016, pp. 4565–4573.